Supporting information for "Effective mass accommodation for partitioning of organic compounds into surface films with different viscosities"

Pascale S. J. Lakey[1,*], Bryan E. Cummings[2], Michael S. Waring[2], Glenn C. Morrison[3] and Manabu Shiraiwa[1,*]

[1] Department of Chemistry, University of California, Irvine, CA 92697, USA.
[2] Department of Civil, Architectural and Environmental Engineering, Drexel University, PA 19104, USA.
[3] Department of Environmental Sciences and Engineering, University of North Carolina, Chapel Hill, NC, USA.

* plakey@uci.edu; m.shiraiwa@uci.edu

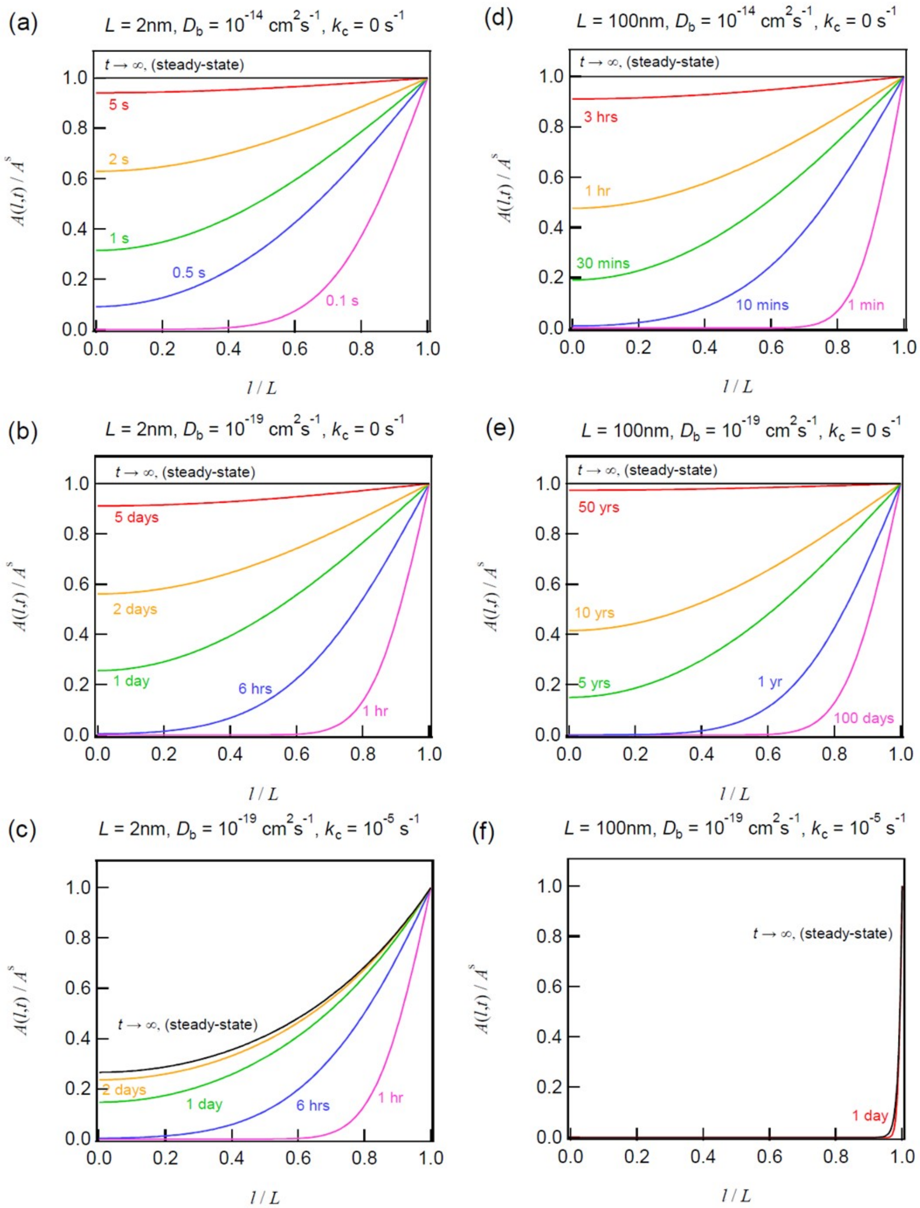

Figure S1: The temporal evolution of the normalized concentration profiles as a function of the normalized distance from the bottom of the film for a (a-c) 2 nm film and (d-f) 100 nm film with different bulk diffusion coefficients and first order reaction rate coefficients; (a) $D_b = 10^{-14}$ cm^2 s^{-1}, $k_c = 0$ s^{-1}, (a) $D_b = 10^{-19}$ cm^2 s^{-1}, $k_c = 0$ s^{-1}, (c) $D_b = 10^{-19}$ cm^2 s^{-1}, $k_c = 10^{-5}$ s^{-1}, (d) various q values which are a function of L, D_b and k_c.

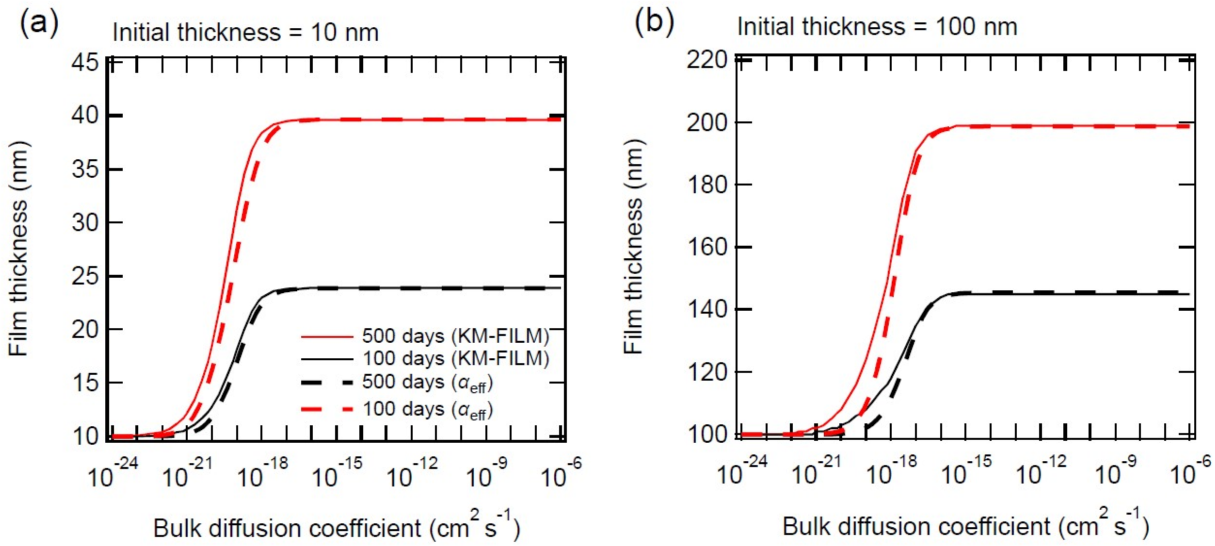

Figure S2: Film thicknesses as a function of bulk diffusion coefficients due to unreactive uptake of SVOCs after 100 days (black lines) and 500 days (red lines) for a film with an initial thickness of (a) 10 nm and (b) 100 nm. C_t is set to 20, 15, 10, 5 and 2 μg m^{-3} for five log K_{oa} bins of unit width centered around 8.5, 9.5, 10.5, 11.5 and 12.5, respectively. Solid lines represent results from the KM-FILM model and dashed lines are results from the α_{eff} model.

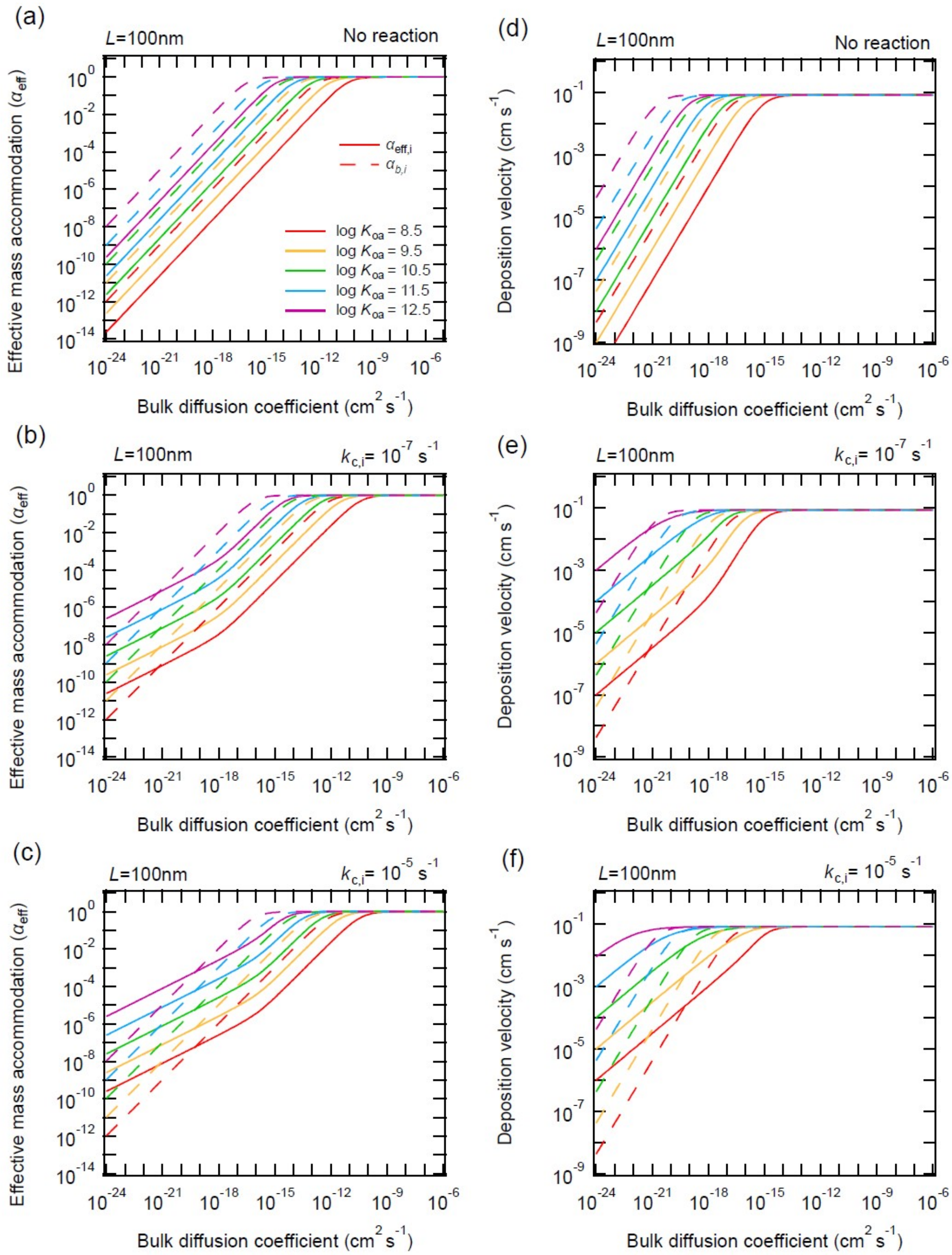

Figure S3: The impact of bulk diffusion coefficients on (a-c) the effective mass accommodation (α_{eff}) and (d-f) the deposition velocity for a film with a thickness of 100 nm and for species with different log K_{oa} values. The pseudo-first order rate coefficient of the different species are set to (a and d) 0 s^{-1} (b and e) 10^{-7} s^{-1} (c and f) 10^{-5} s^{-1}. In panels (a-c) the solid and dashed lines represent α_{eff} and α_b ,respectively, and in panels (d-f) the solid and dashed lines represent the deposition velocity when α_{eff} and α_b are used in equation E1.

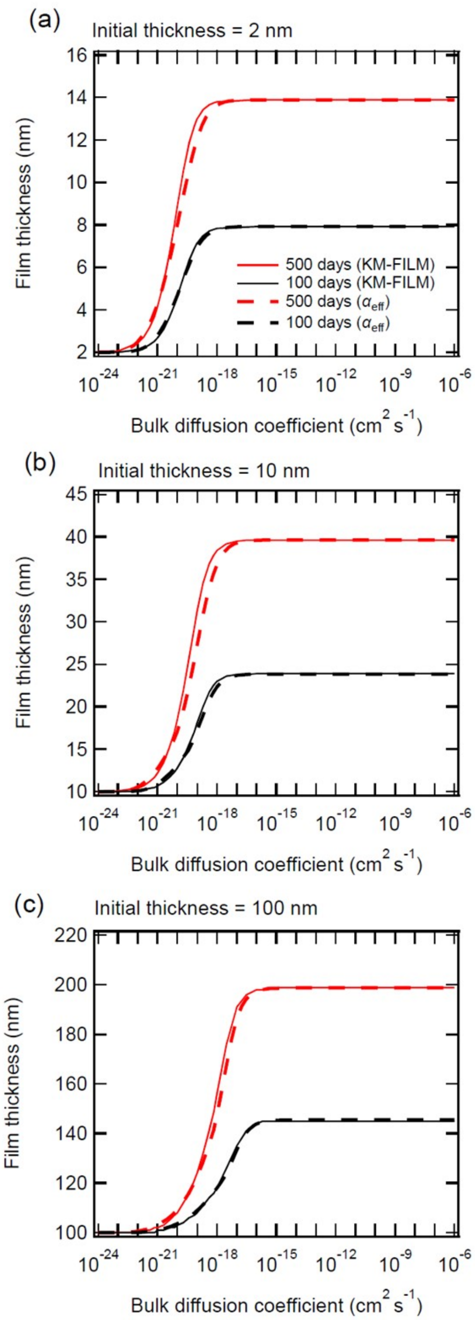

Figure S4: Film thicknesses as a function of bulk diffusion coefficients due unreactive uptake of SVOCs after 100 days (black lines) and 500 days (red lines) for a film with an initial thickness of (a) 2 nm and (b) 10 nm and (c) 100nm. C_t is set to 20, 15, 10, 5 and 2 μg m^{-3} for five log K_{oa} bins of unit width centered around 8.5, 9.5, 10.5, 11.5 and 12.5, respectively. Solid lines represent results from the KM-FILM model and dashed lines are results from the α_{eff} model. In this figure the penetration depth is set to $(D_b t)^{0.5}$ where t is the time unless this exceeds $L/3$.

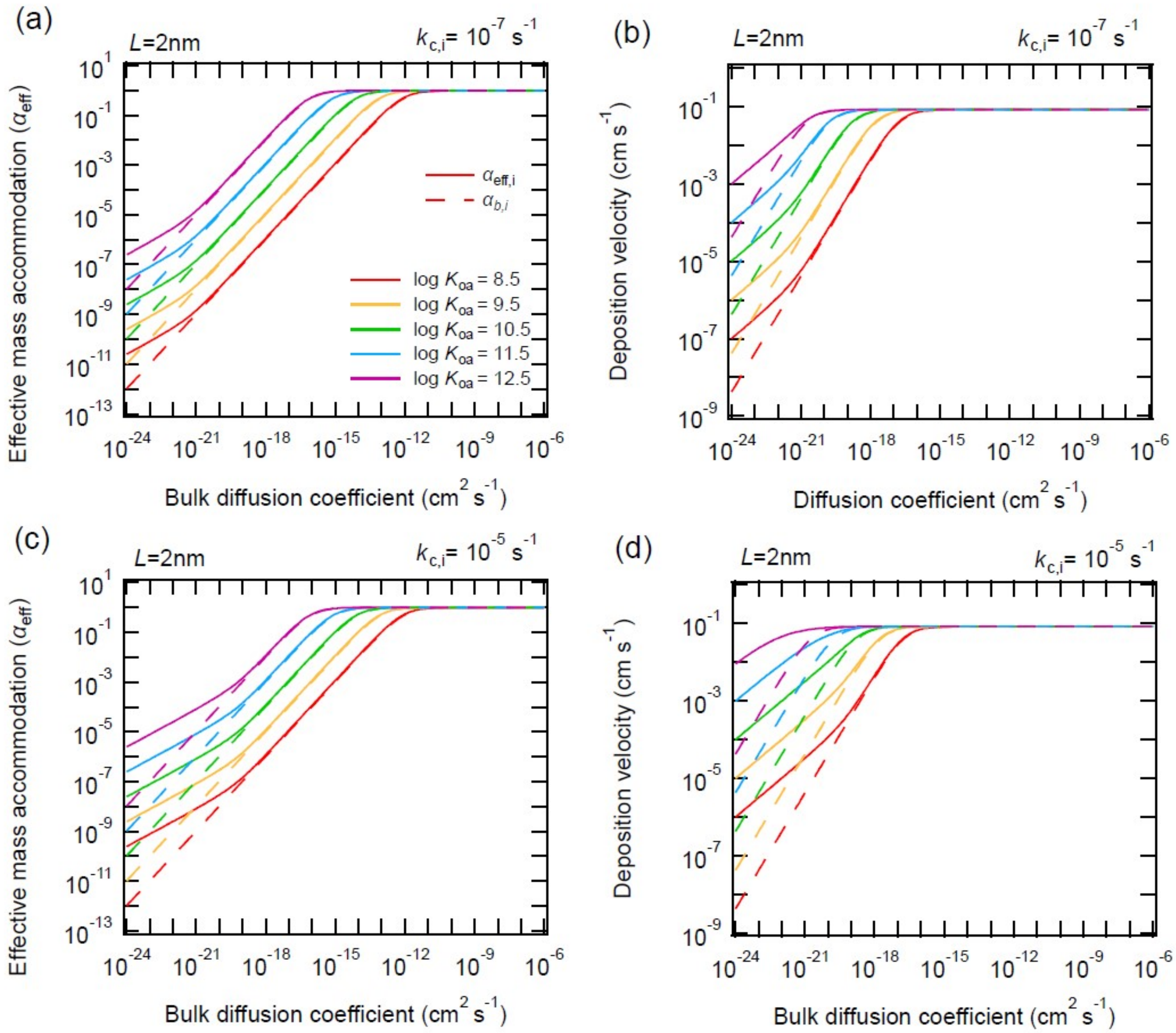

Figure S5: The impact of bulk diffusion coefficients on (a and c) the effective mass accommodation and (b and d) the deposition velocity for a film with a thickness of 2 nm and for species with different log K_{oa} values. The pseudo-first order rate coefficient of the different species are set to (a-b) 10^{-7} s^{-1} (c-d) 10^{-5} s^{-1}. In panels (a-b) the solid and dashed lines represent α_{eff} and α_b, respectively, and in panels (c-d) the solid and dashed lines represent the deposition velocity when α_{eff} and α_b are used in equation E1.

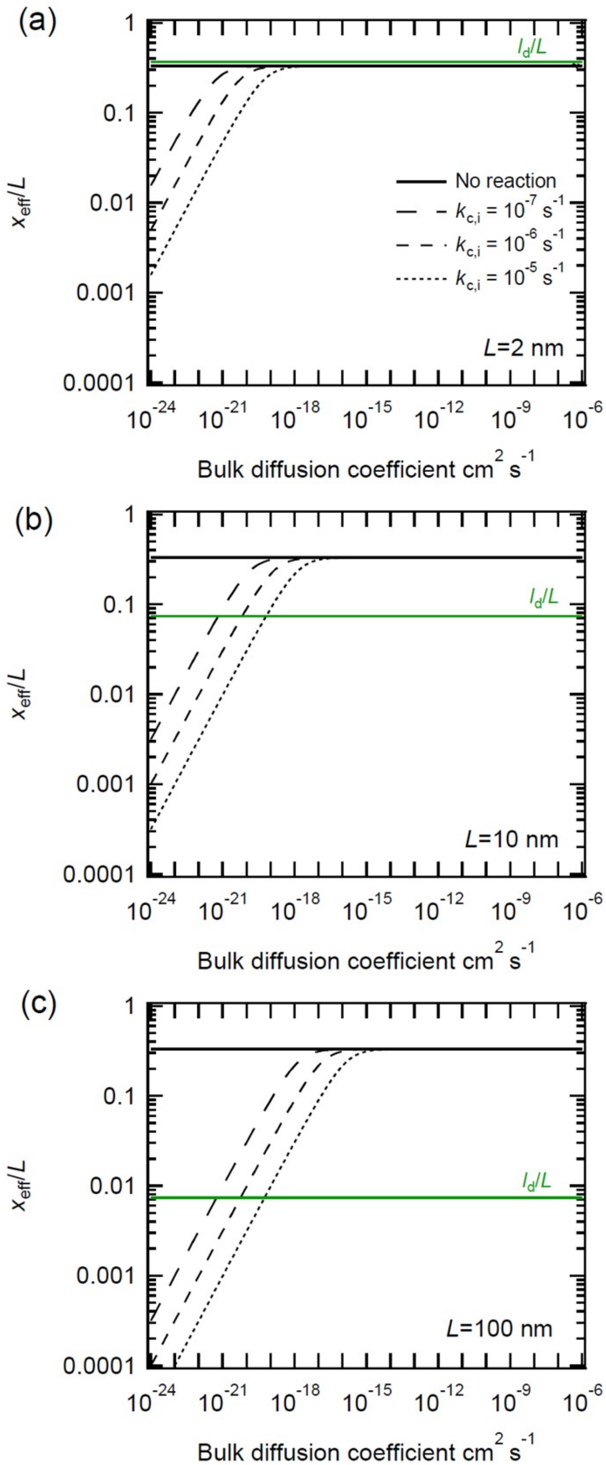

Figure S6: The penetration depth normalized to the total film thickness for different reaction rate coefficients and for a total film thickness of (a) 2nm, (b) 10 nm and (c) 100 nm. The green line shows the distance that a molecule must travel in order to be accommodated into the bulk normalized to the total film thickness.

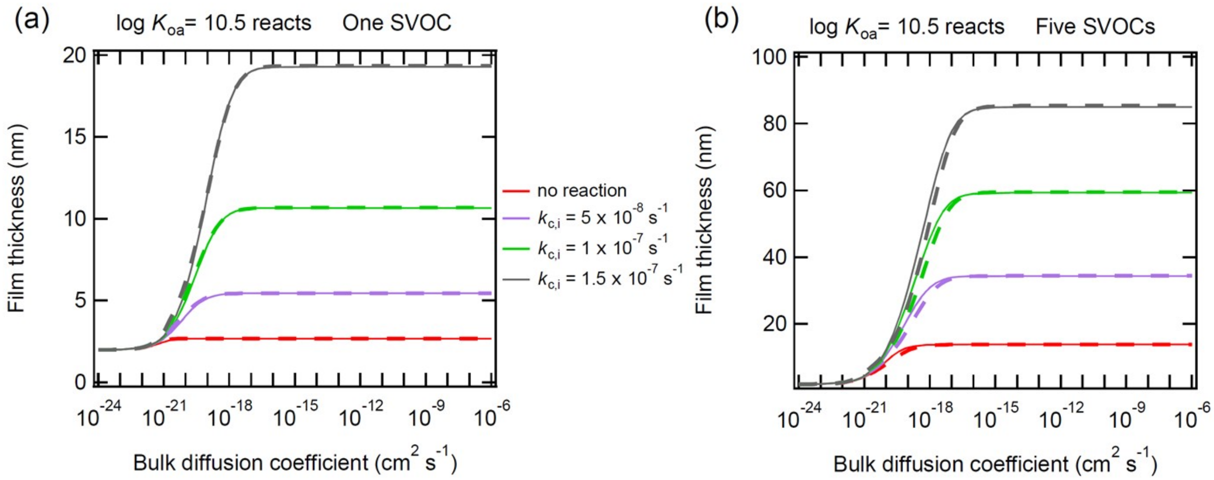

Figure S7: Film thicknesses as a function of bulk diffusion coefficients (D_b) after 500 days for a film with an initial thickness of 2 nm. A range of pseudo-first order reaction rate coefficients are shown for the log K_{oa} bin centered around 10.5. All other species do not react. In panel (a) C_t is set to 10 μg m^{-3} for the log K_{oa} bin centered around 10.5 with the C_t for all other log K_{oa} bins set to 0 μg m^{-3}. In panel (b) C_t is set to 20, 15, 10, 5, and 2 μg m^{-3} for five log K_{oa} bins of unit width centered around 8.5, 9.5, 10.5, 11.5, and 12.5, respectively. Solid lines represent results from the KM-FILM model and dashed lines are results from the α_{eff} model.

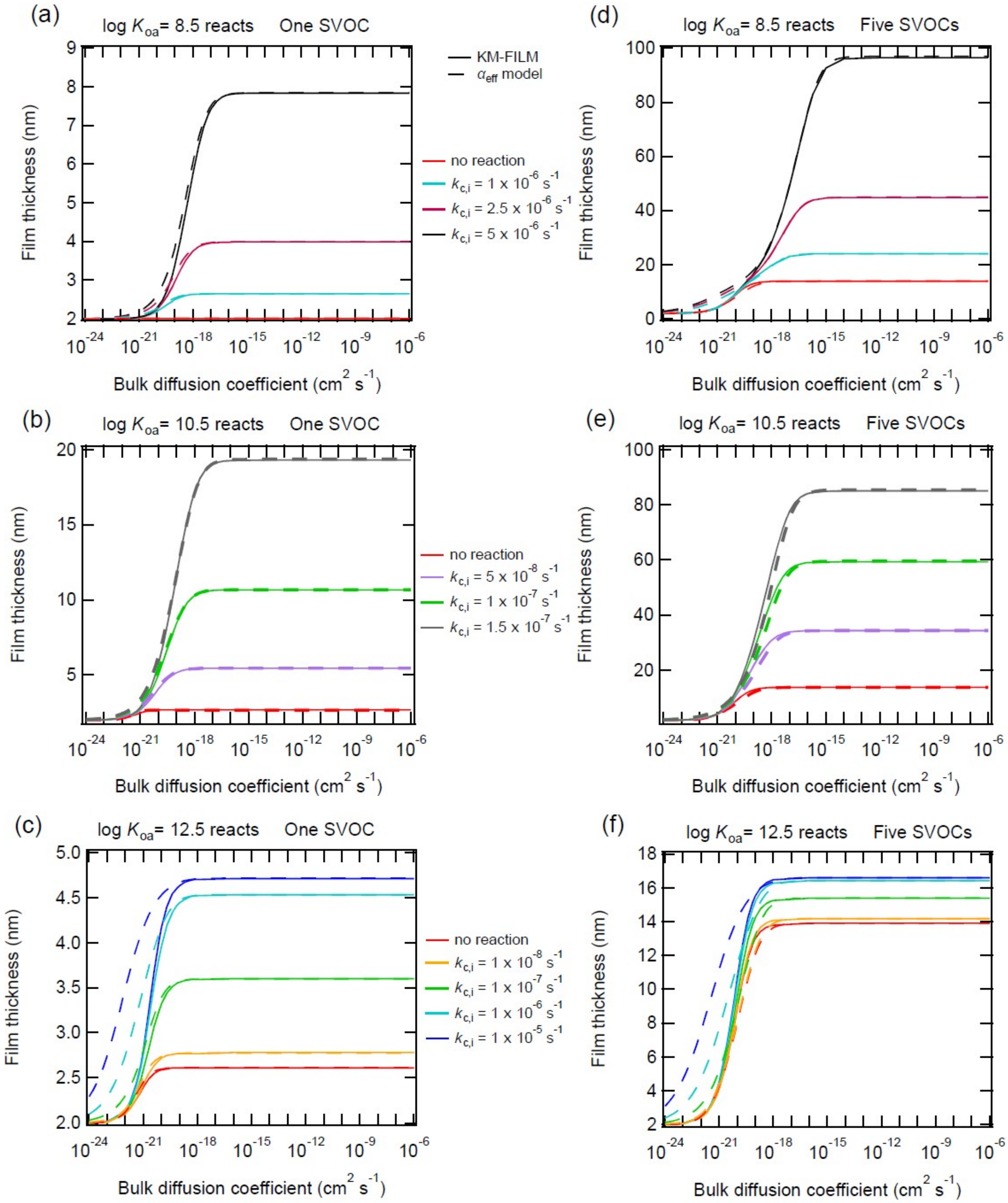

Figure S8: Film thicknesses as a function of bulk diffusion coefficients after 500 days for the conditions shown in Figure 6 and S7. Note that α_{eff} has been used for all simulations even when $\alpha_{eff} > \alpha_b$.

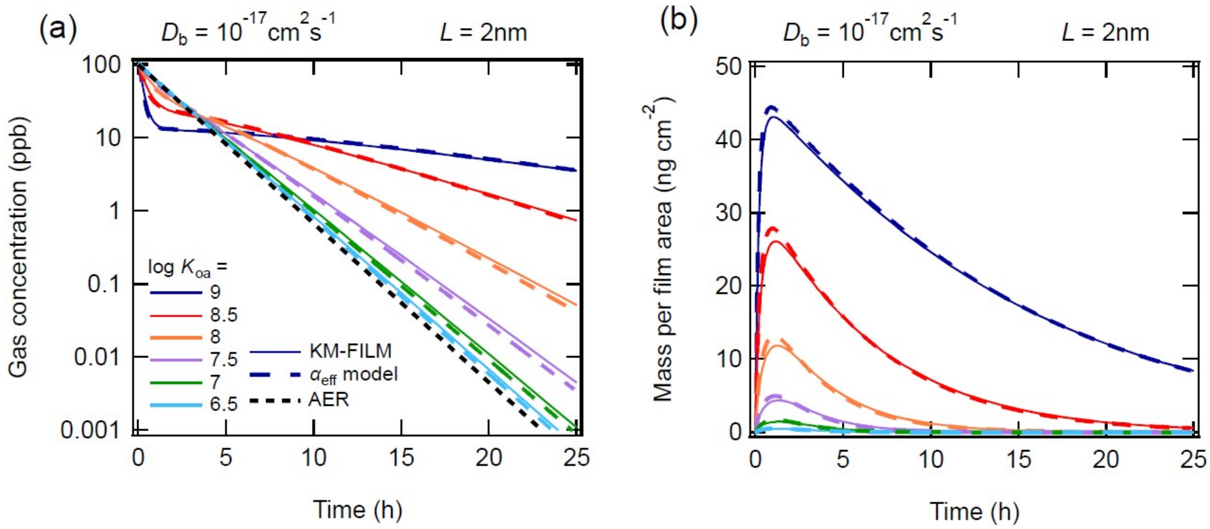

Figure S9: The time evolution of (a) gas-phase concentrations and (b) the mass per film area of SVOCs with different partitioning coefficients after these species are added to a room for five minutes at a constant concentration of 100 ppb. The film thickness is set to 2 nm and the bulk diffusion coefficient is 10^{-17} cm^2 s^{-1}. The air-exchange rate is 0.5 h^{-1} and the surface to volume ratio of the room is 2.5 m^{-1}. Solid lines represent results from the KM-FILM model and dashed lines are results from the α_{eff} model. The dashed black line represents the expected concentration if species are removed at the air-exchange rate.

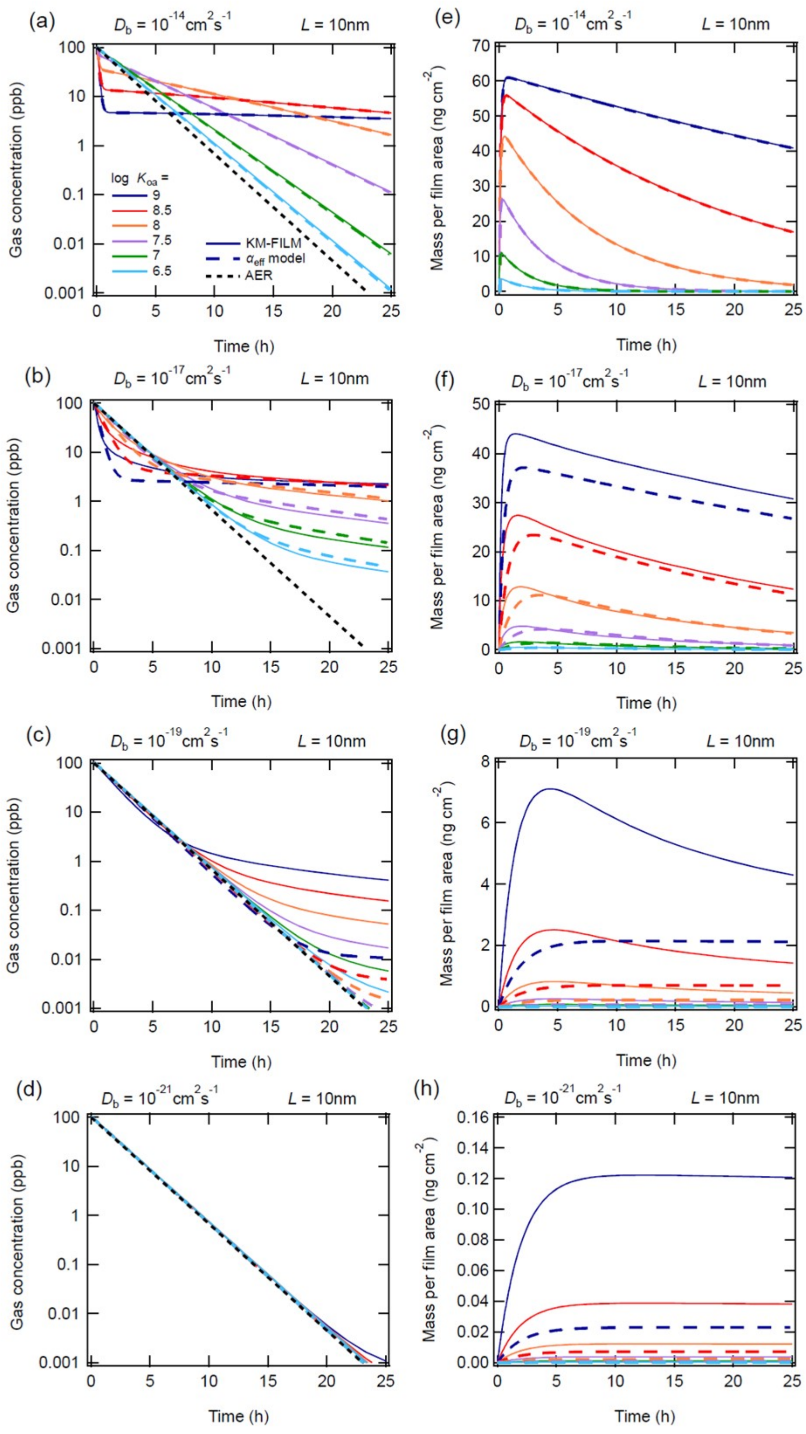

Figure S10: The time evolution of (a-d) gas-phase concentrations and (e-h) the mass per film area of SVOCs with different partitioning coefficients after these species are added to a room for five minutes at a constant concentration of 100ppb. The film thickness is set to 10nm and the bulk diffusion coefficients are (a and e) 10^{-14} cm^2 s^{-1}, (b and f) 10^{-17} cm^2 s^{-1}, (c and g) 10^{-19} cm^2 s^{-1} and (d and h) 10^{-21} cm^2 s^{-1}. The air-exchange rate is 0.5 h^{-1} and the surface to volume ratio of the room is 2.5 m^{-1}. Solid lines represent results from the KM-FILM model and dashed lines are results from the α_{eff} model. The dashed black line represents the expected concentration if species are removed at the air-exchange rate.

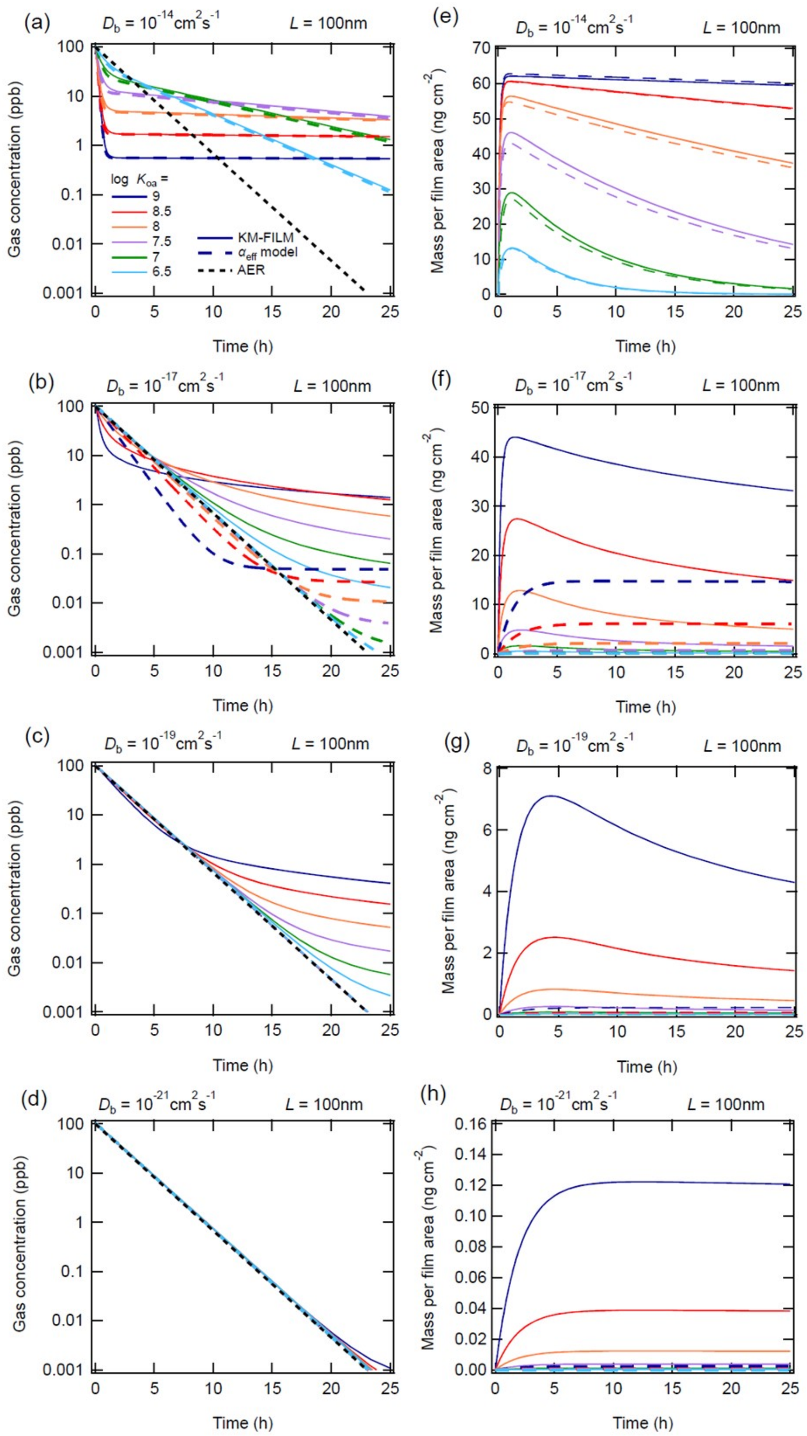

Figure S11: The time evolution of (a-d) gas-phase concentrations and (e-h) the mass per film area of SVOCs with different partitioning coefficients after these species are added to a room for five minutes at a constant concentration of 100ppb. The film thickness is set to 100nm and the bulk diffusion coefficients are (a and e) 10^{-14} cm^2 s^{-1}, (b and f) 10^{-17} cm^2 s^{-1}, (c and g) 10^{-19} cm^2 s^{-1} and (d and h) 10^{-21} cm^2 s^{-1}. The air-exchange rate is 0.5 h^{-1} and the surface to volume ratio of the room is 2.5 m^{-1}. Solid lines represent results from the KM-FILM model and dashed lines are results from the $\alpha_{\rm eff}$ model. The dashed black line represents the expected concentration if species are removed at the air-exchange rate.

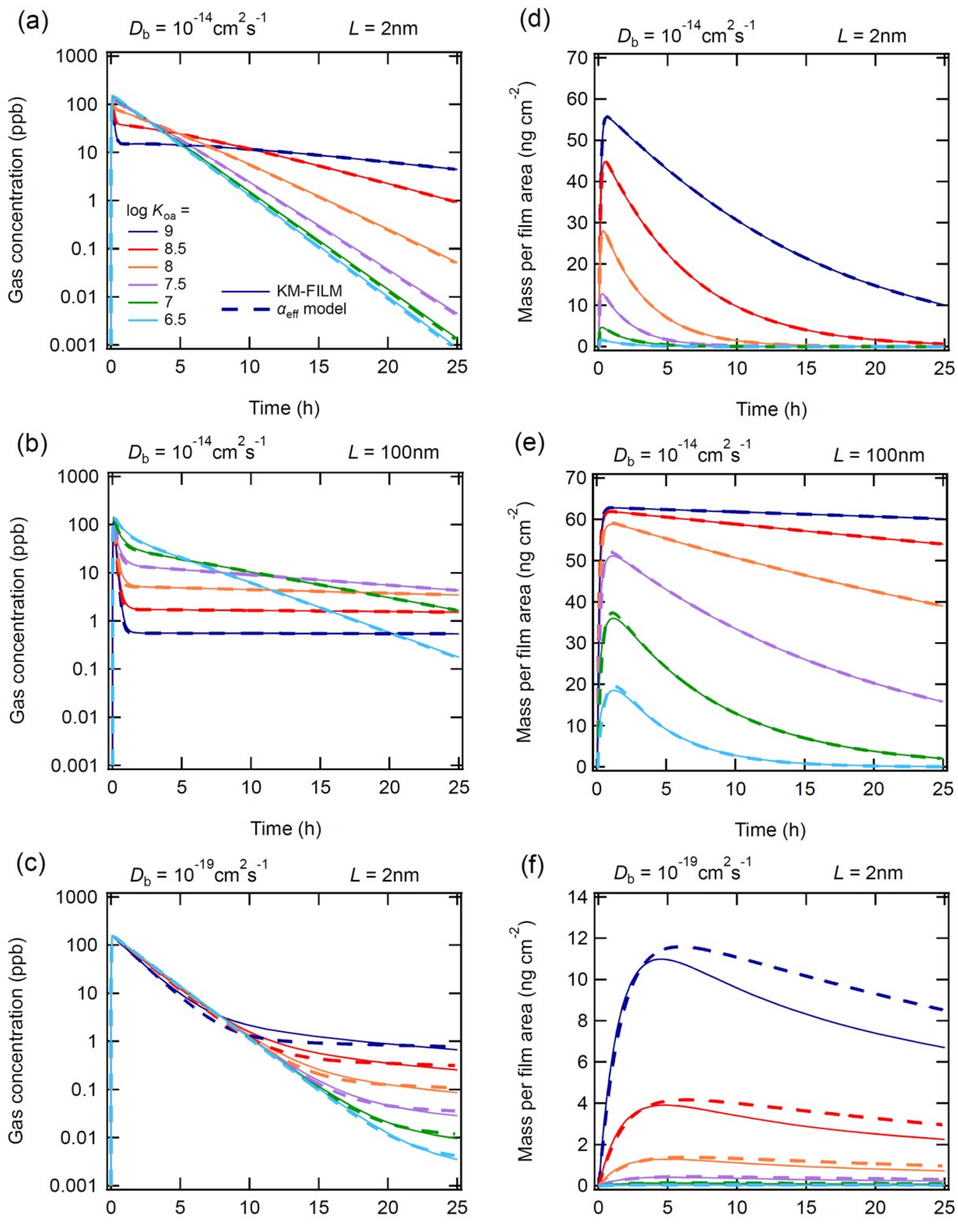

Figure S12: The time evolution of (a-c) gas-phase concentrations and (d-f) the mass per film area of SVOCs with different partitioning coefficients after these species are added to a room at a constant emission rate of 0.55 ppb s^{-1}. The conditions of the simulations are as follows (a and d) $D_b = 10^{-14}$ cm^2 s^{-1}, L = 2 nm, (b and e) $D_b = 10^{-14}$ cm^2 s^{-1}, L = 100 nm, (c and f) $D_b = 10^{-19}$ cm^2 s^{-1}, L = 2 nm.

Tables

Table S1: Parameters used in the models unless specifically stated in the text or figure captions. Note that the parameters for all species are set to the same value unless specifically stated.

Parameter	Description	Value	Comments
α_s	Surface mass accommodation	1	Consistent with molecular dynamic simulations[1, 2]
ω	Mean thermal velocity	1.59×10^4 cm s^{-1}	Calculated for a molecular weight of 250 g mol^{-1}
D_b	Bulk diffusion coefficient	$10^{-24} – 10^{-6}$ cm^2 s^{-1}	See text
L	Film thickness	Various (nm)	See text
l	Distance that molecules adsorbed on the surface must travel to enter the bulk	0.75 nm	Assuming the molecular weight and density shown below
MW	Molecular weight	250 g mol^{-1}	Assumed value
ρ	Bulk-phase density of the molecule, particle or film	1 g cm^{-3}	Assumed value
D_g	Gas diffusion rate coefficient	0.04 cm^2 s^{-1}	Assumed value
ϕ	Boundary layer length next to the surface	0.48 cm	0.04/0.48 = 0.0833 cm s^{-1} = 3 m h^{-1} which is equivalent to the deposition velocity used in Weschler and Nazaroff.[3]
$C_{t,Koa=8.5}$	Total airborne concentration of species with $K_{oa} = 8.5$	20 µg m^{-3} (constant gas-phase concentration model).	This relates only to the constant gas-phase concentration model. Values are for consistency with the Weschler and Nazaroff publication.[4]
$C_{t,Koa=9.5}$	Total airborne concentration of species with $K_{oa} = 9.5$	15 µg m^{-3} (constant concentration model)	
$C_{t,Koa=10.5}$	Total airborne concentration of species with $K_{oa} = 10.5$	10 µg m^{-3} (constant concentration model)	
$C_{t,Koa=11.5}$	Total airborne concentration of species with $K_{oa} = 11.5$	5 µg m^{-3} (constant concentration model)	
$C_{t,Koa=12.5}$	Total airborne concentration of species with $K_{oa} = 12.5$	2 µg m^{-3} (constant concentration model)	
C_g	Gas-phase concentration	Calculated using equation E14 for the constant gas-phase concentration model. Constant 100 ppb for the initial 5 minutes for the changing gas-phase concentration	Assumes a rapid release of a specific chemical compound.

		model.	
TSP	Total airborne suspended particle concentration	20 μg m^{-3}	For consistency with the Weschler and Nazaroff publication.[5]
fom_TSP	Volume fraction of organic matter in the particle	0.4	
S_{room}	Surface area of the room	250 m^2	
V_{room}	Volume of the room	100 m^3	These value give a typical *S*/*V* ratio of 2.5 m^{-1}.[6]
AER	Air exchange rate	0.5 h^{-1}	
k_{gp}	First-order gas-particle mass transfer coefficient	0 s^{-1}	Typical value for a residential home.[7, 8]
k_g	Pseudo-first-order chemical reaction rate coefficient in the gas-phase	0 s^{-1}	For simplicity when running the model
C_{out}	The concentration outside of the room	0 μg m^{-3}	
E	Emission rate inside the room	0 μg m^{-3} s^{-1} or ppb s^{-1} unless otherwise stated	

Table S2: Peak gas-phase concentrations and mass per film area for species with a log K_{oa} of 9 and 6.5. Simulations were performed with different D_b and *L* values and either a constant 100 ppb concentration or an emission rate of 0.55 ppb s^{-1} over the first five minutes.

Conditions	**Peak gas-phase concentration (ppb) (emission rate of 0.55 ppb s^{-1})**	**Peak mass per film area (ng cm^{-2}) (emission rate of 0.55 ppb s^{-1})**	**Peak mass per film area (ng cm^{-2}) (constant 100 ppb conditions)**
$D_b = 10^{-14}$ cm^2 s^{-1} *L* = 2 nm	121 (log K_{oa} = 9) 157 (log K_{oa} = 6.5)	55.6 (log K_{oa} = 9) 1.6 (log K_{oa} = 6.5)	55.0 (log K_{oa} = 9) 1.0 (log K_{oa} = 6.5)
$D_b = 10^{-14}$ cm^2 s^{-1} *L* = 100 nm	120 (log K_{oa} = 9) 149 (log K_{oa} = 6.5)	62.8 (log K_{oa} = 9) 18.6 (log K_{oa} = 6.5)	62.1 (log K_{oa} = 9) 13.2 (log K_{oa} = 6.5)
$D_b = 10^{-19}$ cm^2 s^{-1} *L* = 2 nm	159 (log K_{oa} = 9) 160 (log K_{oa} = 6.5)	11.0 (log K_{oa} = 9) 0.04 (log K_{oa} = 6.5)	7.1 (log K_{oa} = 9) 0.03 (log K_{oa} = 6.5)

References

1. M. von Domaros, P. S. Lakey, M. Shiraiwa and D. J. Tobias, Multiscale Modeling of Human Skin Oil-Induced Indoor Air Chemistry: Combining Kinetic Models and Molecular Dynamics, *J. Phys. Chem. B*, 2020, **124**, 3836-3843.
2. J. Julin, P. M. Winkler, N. M. Donahue, P. E. Wagner and I. Riipinen, Near-unity mass accommodation coefficient of organic molecules of varying structure, *Environ. Sci. Tech.*, 2014, **48**, 12083-12089.
3. C. J. Weschler and W. W. Nazaroff, Growth of organic films on indoor surfaces, *Indoor Air*, 2017, **27**, 1101-1112.

4. M. Shiraiwa, C. Pfrang and U. Pöschl, Kinetic multi-layer model of aerosol surface and bulk chemistry (KM-SUB): the influence of interfacial transport and bulk diffusion on the oxidation of oleic acid by ozone, *Atmos. Chem. Phys.*, 2010, **10**, 3673-3691.
5. G. Morrison, P. S. Lakey, J. Abbatt and M. Shiraiwa, Indoor boundary layer chemistry modeling, *Indoor Air*, 2019, **29**, 956-967.
6. A. Manuja, J. Ritchie, K. Buch, Y. Wu, C. M. Eichler, J. C. Little and L. C. Marr, Total surface area in indoor environments, *Environ. Sci.: Processes Impacts*, 2019, **21**, 1384-1392.
7. N. Yamamoto, D. Shendell, A. Winer and J. Zhang, Residential air exchange rates in three major US metropolitan areas: results from the Relationship Among Indoor, Outdoor, and Personal Air Study 1999–2001, *Indoor Air*, 2010, **20**, 85-90.
8. M. Yao and B. Zhao, Distribution of air change rates in residential buildings in Beijing, China, *Proceedings of the 11th International Symposium on Heating, Ventilation and Air Conditioning (ISHVAC 2019) Volume I: Indoor and Outdoor Environment 11*, 2020, 1149-1156.